Tidal effects on acoustic propagation off eastern Australia

Robin ROBERTSON[1];Paul HARTLIPP[1]

[1] University of New South Wales Canberra @ ADFA, Australia

ABSTRACT

Sound propagation in the waters off Eastern Australia is of keen interest to the Royal Australian Navy (RAN) as it affects sonar operation in one of their prime operating regions. Using temperature and salinity fields from an internal tidal model to determine horizontally and vertically dependent sound velocities, effects of internal tides on sound propagation were investigated along four latitude transects across the continental shelf into the deep basin off Eastern Australia. The sound velocity fields and individual acoustic ray paths varied during both the daily and spring-neap tidal cycles, although their basic characteristics were similar. The most noticeable tidal effects were for sound channel formation. More acoustic rays were present in the mid-water column sound channels over both the continental shelf and in the deep basin during spring tide than neap tide and there was a stronger latitude dependence on this number of rays. However, most of the metrics used to evaluate the acoustic rays did not show appreciable differences for either the spring-neap or the daily tidal cycles. There were strong dependencies of these metrics on latitude and source depth. Here, tidal effects on acoustic propagation appear overpowered by effects from other features such as currents and eddies.

Keywords: acoustic Propagation, Internal Tides, Internal Waves
I-INCE Classification of Subjects Number(s): 54.3

1. INTRODUCTION

Propagation of acoustic rays in the ocean depends on temperature, salinity, and density (Frosch 1964). While pressure is primarily controlled by depth, temperature and salinity vary in the ocean due to currents, the surface mixed layer, eddies, internal waves and other oceanographic features. These features affect the structure of the temperature and salinity fields, which in turn determines the sound velocity fields. Furthermore, these features change both in time and space, modifying the temperature, salinity and sound velocity fields spatially and temporally too. Effects of eddies and the surface mixed layer were investigated by Jones et al. (2013). Using BLUElink model results for the temperature fields, they found that eddies induce a highly variable sound velocity field, which affected surface duct transmission. Another oceanographic feature which affects acoustic propagation are internal tides and waves.

Internal tides are waves internal to the ocean with a tidal frequency. As they propagate they alter the temperature structure and consequently the sound velocity fields. Fluctuations of the isotherms by internal tides often are of the order of 50 m in the thermocline around 500 m depth and 100's of m deeper in the ocean where the density stratification is weaker. Internal tides are generated by interactions of the tide with topographic features, such as the continental shelf, seamounts, etc. Energy from the internal tides also shifts from the tides to other frequencies as internal waves through non-linear interactions. Although an "internal calm" has never been observed, the internal wave field varies during both the daily and spring-neap tidal cycles, resulting in an intermittency in their influence on the temperature, salinity, and sound velocity fields.

In areas of active internal tides, such as Australia's North West shelf, the South China Sea, or the Indonesian seas, very large, non-linear internal waves are generated. The "episodic nature of packets of internal waves gives intermittency to some acoustic effects" and affects acoustic propagation (Duda 2013). Using temperature and salinity fields for Ombai Strait from a tidal model for the Indonesian seas, Cooper (2011) found that a sound channel around 500 m formed and disappeared during both the

[1] r.robertson@adfa.edu.au

daily, twice-daily, and the spring-neap tidal cycles. The number of rays trapped within the sound channel fluctuated with the tides. The limits of the upper and lower limiting rays also fluctuated with the tidal cycles. So in Ombai Strait, there was a strong tidal dependence of the acoustic propagation.

In order to investigate the effects of internal waves on acoustic propagation in the waters off eastern Australia, acoustic rays were traced over transects along four different latitudes with five different source depths (2 m, 20 m, 50 m, 200 m, and 500m), using temperature fields from a tidal simulation (Figure 1) (Hartlipp and Robertson 2014).

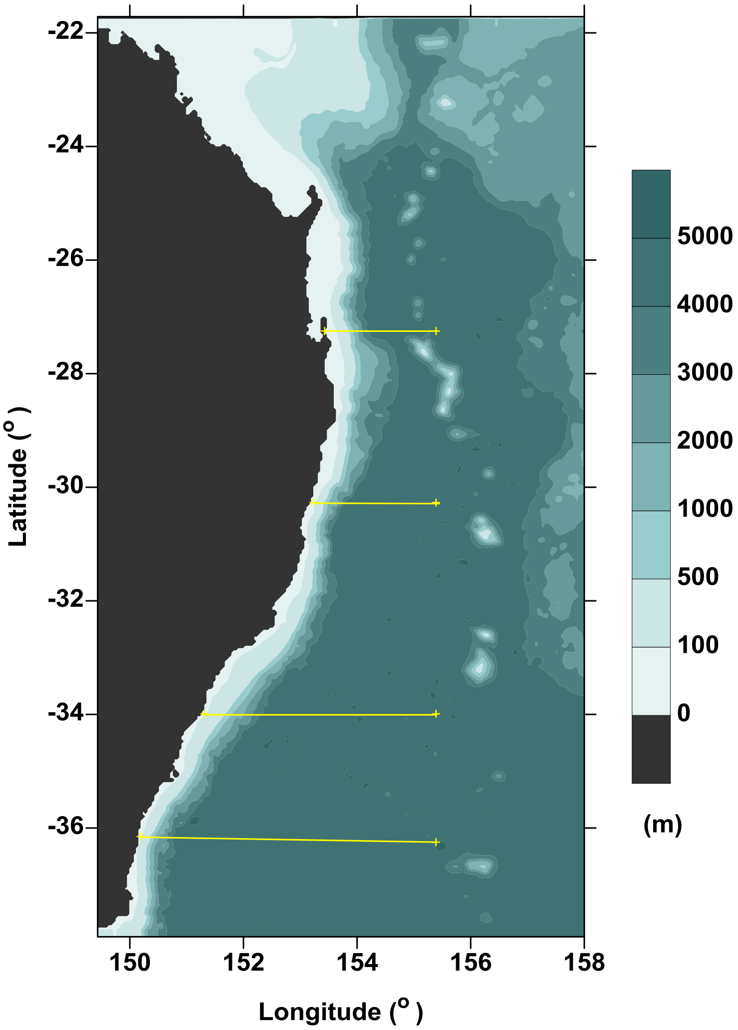

Figure 1 – The location of the four cross-shelf transects used for investigating acoustic wave propagation are indicated by yellow lines, with the start location on the left. The background is the bathymetry off the East coast of Australia. The entire domain of the simulation is not shown.

2. RAY TRACING

The acoustic rays were traced using Dushaw's eigenray program (Dushaw and Colosi 1998). This program traces acoustic rays along a 2-D sound speed field, which varies both horizontally and vertically. It was designed to "achieve fast, accurate wavefront, and eigenray travel time predictions" and is based on Bowlin's RAY program (Dushaw and Colosi 1998). At the source depth, 40 rays with originating angles ranging from -45° to 45° were started for source depths below 2 m. For the 2 m source depth, the angles ranged only from -45° to 0°. For our use here, all rays were traced and included in the analysis without regard to receiver depth and a relatively high number of bounces, 50, were allowed. It is recognized that the individual rays would likely dissipate before this number of bounces occurred. However, since the purpose here was to look at propagation over the entire shelf region, it was decided to have one ray with lots of bounces instead of performing several runs for the same sound speed map, but with different longitudes across the continental shelf or slope for the source locations. The source location was 6 km from the coast for shallow source depths and over the continental slope for the deep source depths.

3. SOUND SPEED FIELDS

To provide sound speeds for the waters off eastern Australia, potential temperature and salinity fields during the tidal cycles were determined using temperature and salinity data from a tidal model of the region (Hartlipp and Robertson 2014). The hydrodynamic model used was the Regional Ocean Modelling System (ROMS). ROMS was run for 60 days at a 4 km resolution with realistic hydrography and tidal forcing. Incoming solar radiation was not included in the simulation. The model and simulations, including comparisons to observations, are described more fully in Hartlipp and Robertson (2014).

Transects of these hydrographic fields across the continental shelf and slope into the deep basin were used to calculate sound speed profiles at 4 km horizontal intervals. The UNSESCO algorithms for pressure and sound velocity were used to convert depth to pressure and calculate the sound speed from the potential temperature, salinity and pressure fields (Fofanoff and Millard 1983). Since potential temperature varies with latitude, sound speed fields were investigated along transects across the continental shelf into the deep basin at four different latitudes (Figure 1).

Sound speed fields were generated at hourly intervals along each of the four latitude transects (Figures 2b-e and Figure 3). Seven 48 hour period including both spring and neap tides were selected for this study and are indicated on the elevation time series in Figure 2a. Transects of the sound velocity at 34°S are shown for 3 different hours spaced 6 hours apart during both spring and neap tides are shown in Figure 3. The basic structure of the sound velocity is similar for all hours; however,

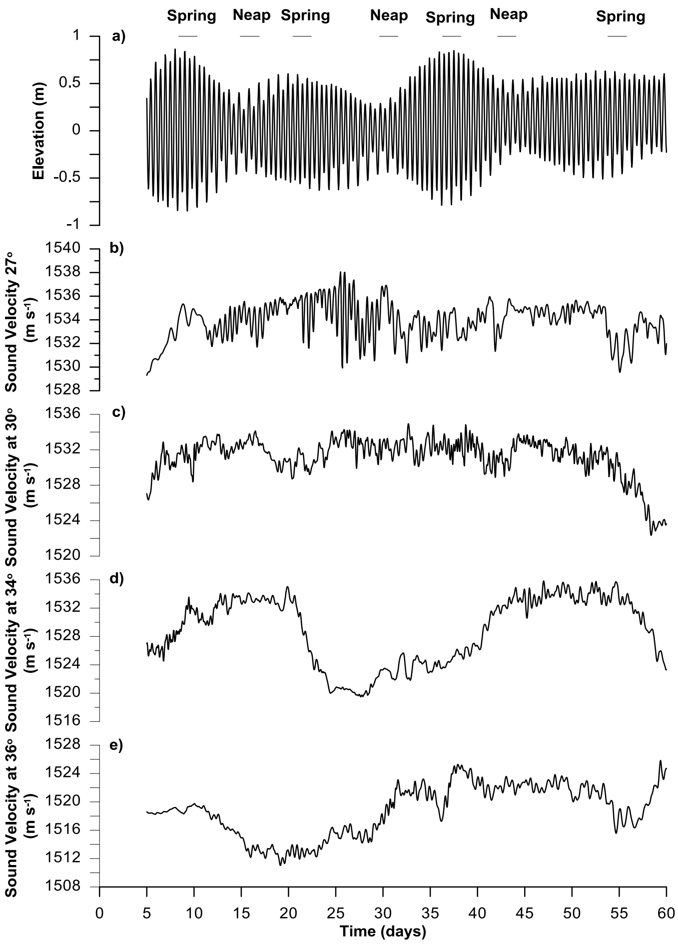

Figure 2 – a) Time series of the elevation over the continental shelf at 27°S from the simulation. Elevation time series at the other latitudes are similar. Time series of the sound velocity profile near the surface for the four transects across the continental shelf are shown roughly at b) 27°S, c) 30°S, d) 34°S, and e) 36°S

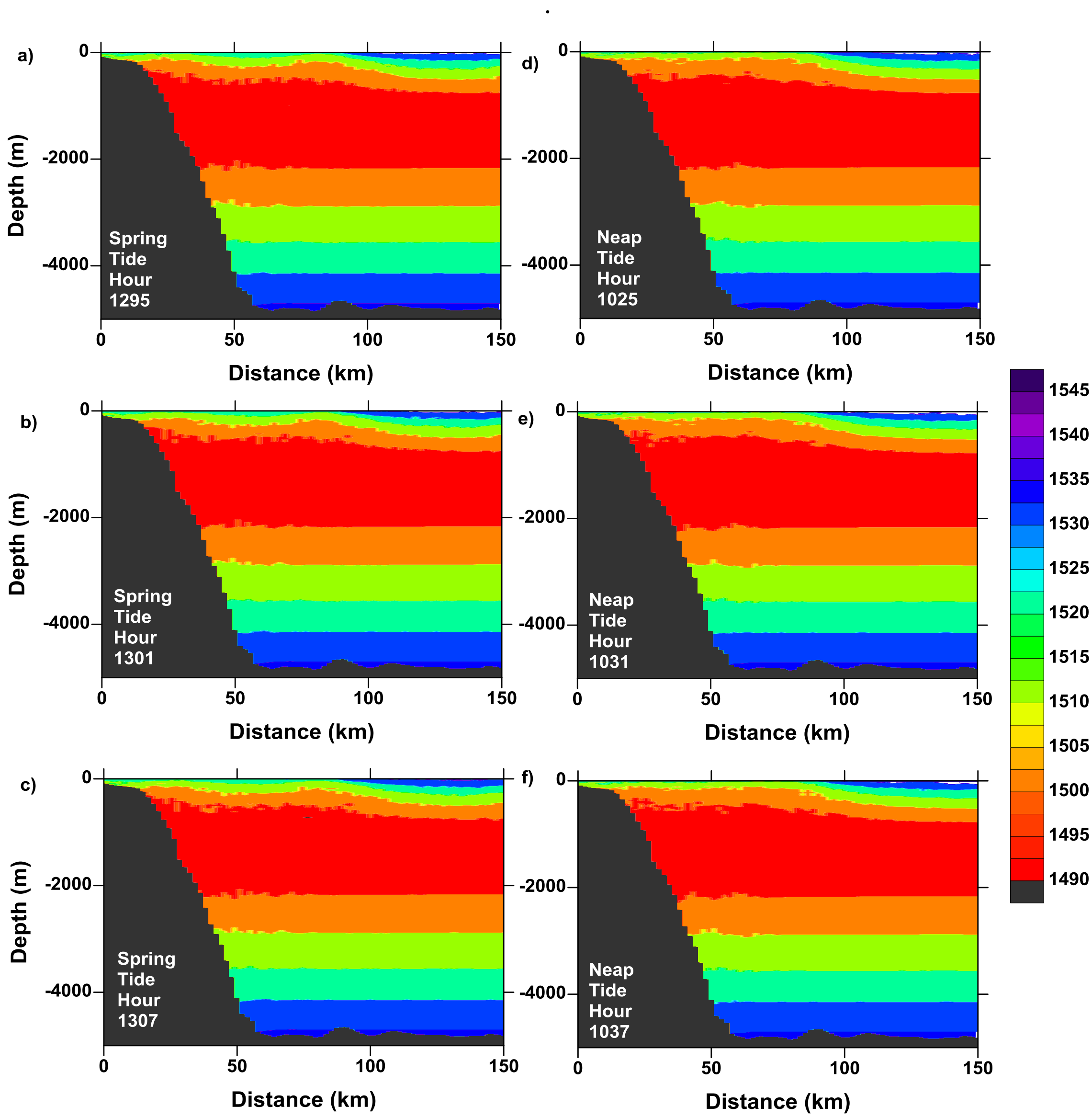

Figure 3 – Transects of the sound velocity field at 34ºS during spring a-c) and neap tide d-f).

small differences occur due to tides and other processes. Although the model was only forced with tides, the realistic hydrography generated a strong, southward geostrophic current, ~ 1.5 m s^{-1}, near the coast, a weaker northward flow offshore, and many eddies, resulting in a relatively complex background flow.

4. SENSITIVITY OF THE ACOUSTIC PROPAGATION RAYS

Acoustic rays were traced for sound fields from both the selected spring and neap tidal periods along each of the four latitude transects and for each of the five source depths. Acoustic rays were traced for total of 13,440 cases with different sound velocity fields or source depths. Analysis and synthesis of the analysis for this large number of cases required development of some metrics to evaluate the resultant ray fields. The typical features used to describe acoustic propagation are surface ducts, sound channels, convergence zones, shadow zones, and the upper and lower limiting ray or upper and limiting turning depths. For our metrics, we used the number of rays, surface ducts, the upper and lower turning depths, and sound channels. Although all cases, started with 40 rays, the number of rays differs between cases because some were dropped due to an excessive number of bounces. Surface ducts were identified for three depths: 10, 20 and 50 m over the continental shelf and 20, 50, and 1000 m in the deep basin. The formation of “surface” ducts was inhibited by neglecting incoming solar radiation and consequently the "afternoon" effect. So the "surface" ducts are not a result of sound speed change but of the ray not penetrating the thermocline. The ray diagrams were also diagnosed for sound channels, where the rays propagate within a narrow depth band. Over the continental shelf, sound channels were searched at 20m$\pm$10m, 50m$\pm$20m, 100m$\pm$50m, and 200m$\pm$10m. In the deep basin, sound channels were additionally searched at 1500m$\pm$500m and 1500m$\pm$1000m. The upper and lower turning depths for each ray were determined by Dushaw's software. Although convergence zones and shadow zones were observed in the ray diagrams, no metrics for them were developed. There was no metric for critical rays.

The behavior of the acoustic rays differed drastically between the continental shelf and the deep basin. Over the continental shelf, rays typically bounced from the surface to the bottom, although some stayed near the bottom in roughly a "surface" duct and other remained near the bottom in a "bottom" duct. The thermocline acted as a barrier for these rays, with the effectiveness of it as a barrier dependent on the angle of the ray as it reached the thermocline. As a result, analysis for these two regions were separated, for the shallow source depths.

The ray paths were observed to change each hour for all source depths and all latitude transects. Some examples of rays at different hours from a source depth of 20 m at 30^{o}S are shown in Figure 4 for spring tide and Figure 5 for neap tide. Like the basic sound velocity fields, the acoustic rays as a whole follow similar paths; however individual rays follow different paths. Differences exist, particularly in deeper water. During spring tide, one ray goes much deeper than in the water column than the others (Figure 4a). This occurred often. Six hours later, there are several rays that oscillate much closer to 1000 m, within 100 m, than most of the rays with 1000 m fluctuations (Figure 4b). These tightly fluctuating rays disappear 6 hours later (Figure 4c). During neap tide, the same general pattern is followed (Figure 5); however, there is less difference in both the sound velocities (not

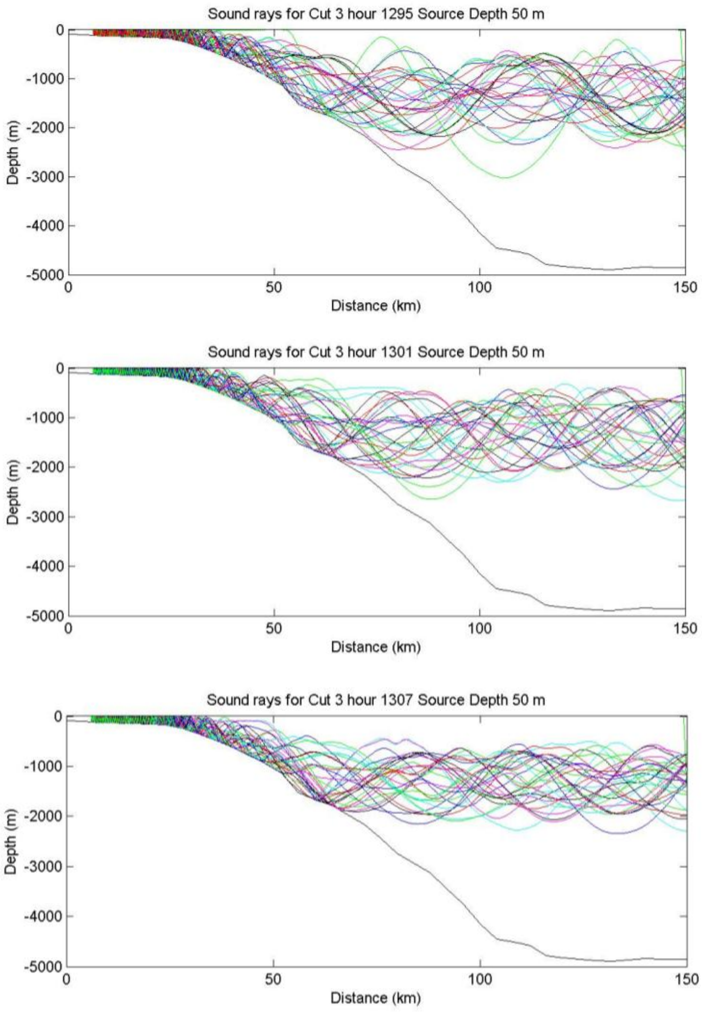

Figure 4 – Paths of acoustic rays along the 34^{o}S transect during spring tide for hours 1295 (top panel), 1301 (middle panel) and 1307 (bottom panel). The bottom is represented by a black line.

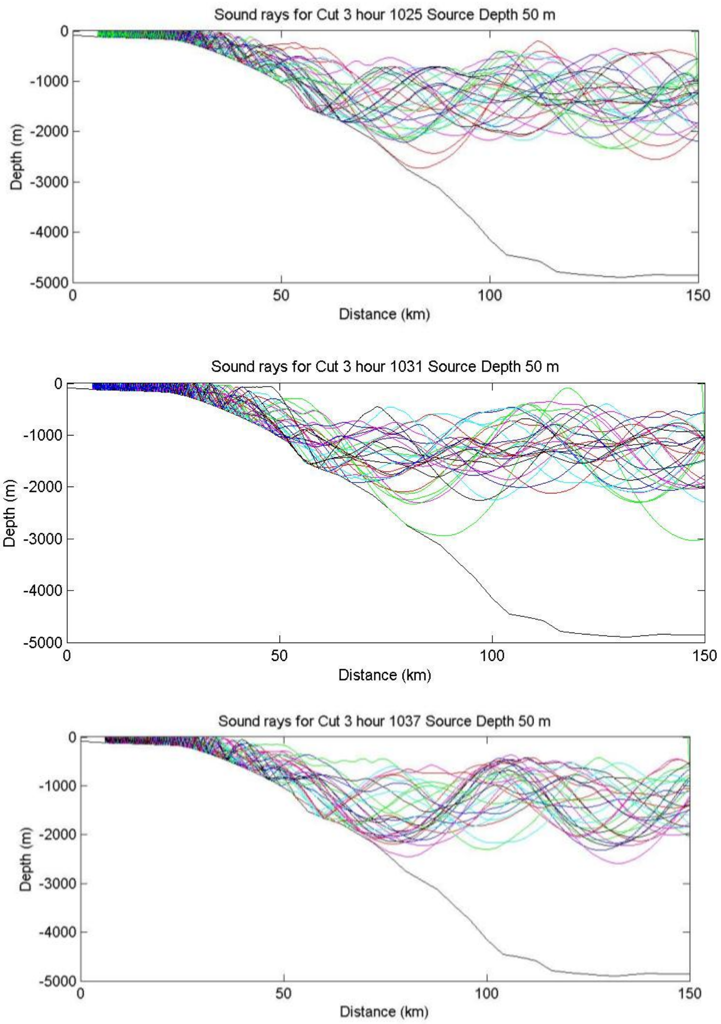

Figure 5– Paths of acoustic rays along the 34^{o}S transect during neap tide for hours 1025 (top panel), 1031 (middle panel) and 1037 (bottom panel). The bottom is represented by a black line.

shown) and the acoustic ray paths with time. More rays with the larger fluctuations occur and fewer with the tighter fluctuations. Further dependencies of the acoustic ray behavior on latitude and the tidal cycles are outlined below for the primary metrics.

4.1 Number of Rays

The number of rays varied with latitude. The northernmost transect (27^{o}S) lost about 50% of the rays to excessive bounces (Figure 6b and g). The southernmost transect (36^{o}S) and the 30^{o}S transect lost the fewest rays with the 34^{o}S transect falling in between the others. There was no appreciable difference in the number of rays between the spring and neap time periods, although there was slightly more variability during spring tide. These patterns were consistent for all source depths.

4.2 Surface Ducts

There was no appreciable change in the number of rays limited to the upper 20, 50, or 100 m over the continental shelf for the spring-neap or daily tidal cycles (Figure 6c and h). Also a latitude dependence was not apparent. Solar radiation was not included in order to isolate the tidal effects. However, without solar radiation changing the sound velocity at the surface, a true surface duct was not formed. So it is not surprising that there is no dependence of surface ducts on the tide.

4.3 Sound Channels

Sound channel formation both over the continental shelf and the deep basin were affected by the spring-neap tidal cycles (Figure 6d and 6i and Figure 6e and 6j, respectively). At 34^{o}S over the continental shelf, there were more acoustic rays in the sound channel around 100 m during spring tide (Figure 6d) than neap tide (Figure 6i). However, the number of rays in this channel is not statistically significant. The response in the deep basin is much stronger. For the wider, deep sound channel, within 1000 m on either side of 1500 m, the number of rays within the sound channel varied more with latitude during spring tide (Figure 6e) than during neap tide (Figure 6j). Spring tide showed a strong latitude dependence, with the more acoustic rays in the sound channel at 34°S and the fewer at 36°S and more consistency. There were approximately the same number of rays at 27 °S and 30°S.

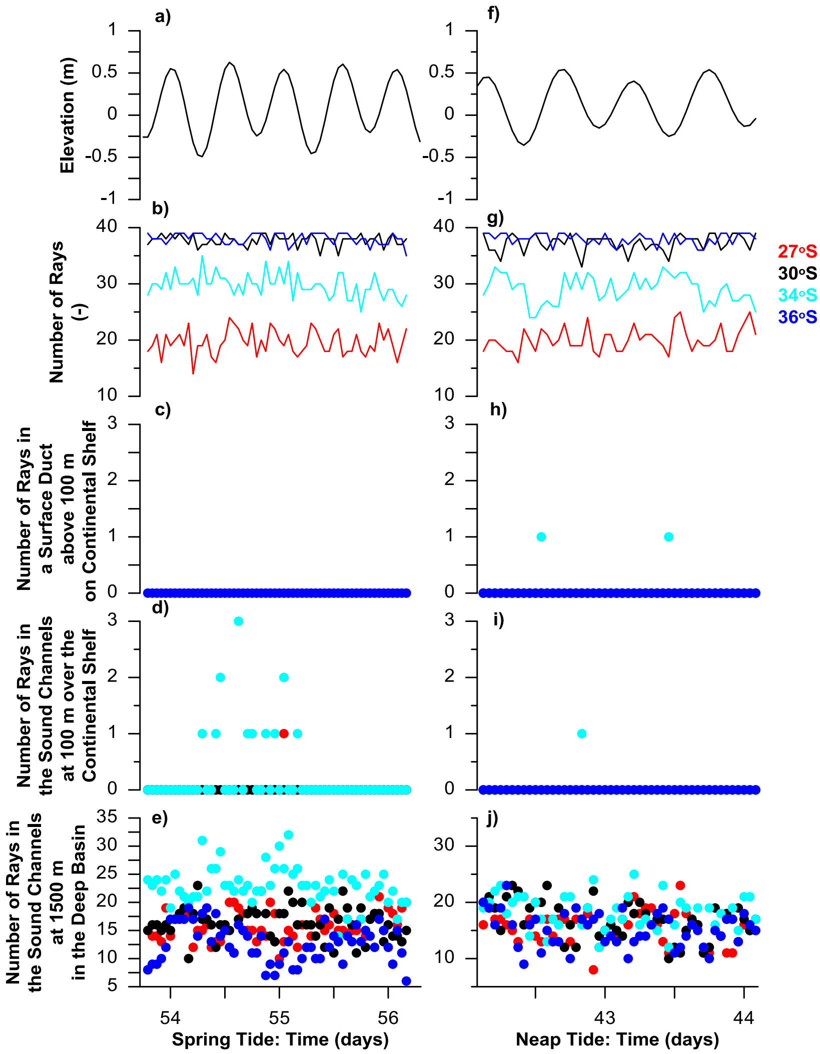

Figure 6 – Time series of the elevation over the continental shelf at 27°S from the simulation for the a) spring and f) neap time periods. The number of rays which progressed through the transect with less than 50 bounces for the b) spring and g) neap time periods for a source depth of 50 m. The number of rays which fall in the surface duct from 0-100 m over the continental shelf are shown for the c) spring and h) neap time periods. The number of rays which fall in a sound channel centered on 20 m ranging from 10-30 m over the continental shelf are shown for the d) spring and i) neap time periods. The number of rays which fall in a sound channel centered on 1500 m ranging from 500-2500 m over the deep basin are shown for the d) spring and j) neap time periods. The transects at the different latitudes in the different panels are indicated by red for 27°S, black for 30°S, cyan for 34°S, and blue for 36°S

5. DISCUSSION AND SUMMARY

There were strong dependencies on both latitude and source depth. Various metrics changed with latitude, but not in linear manner either from North to South or South to North. Typically, the behavior at 36°S and 30°S was similarly and the then changed to 34° S and 27°S, depending on the metric, as discussed earlier. We recognize that part of the latitude dependence resulted from different topography along the transects. Since the two deeper source depths originated over the continental shelf and did not cover the same region, source depths were broken into two groups: shallow source depths, 2, 20, and 50 m and deep source depths, 200 and 500 m. Some metrics, such as the number of rays, were essentially the same for the shallow source depths. Others, such as the sound channels over the shelf, showed a stronger spring-neap tide response with increasing source depth from 2 to 50 m. Rays emanating from the deeper source depths were also dependent on latitude and showed more variation than those from the shallow sources, primarily due to the increased water depth.

Although the individual ray paths changed each hour and the sound velocity time series show definite daily and spring-neap tidal cycles, the general behavior for the group of sound waves was relatively similar for a particular latitude transect and source depth. In other words, most of the metrics did not vary appreciably with either the daily or spring-neap tidal cycle off eastern Australia, as they did for Ombai Strait in the Indonesian seas. The exception is the sound channels in the deep basin and to a lesser extent over the continental shelf, where the spring-neap cycle was apparent. There was a stronger latitude dependence in the number of rays in the deep sound channel, 1000 m on either side of 1500 m depth, in the deep basin during spring tide. There were more sound rays during spring tide at 34°S and fewer at 36°S and there was a more consistent pattern for the number of rays in the sound channels during spring tide. For the shallow sound channels, more rays were in sound channels in the around 20, 50, 100, and 500 m for sources at 20 and 50 m and for 100 and 500 m for sources at 2 m.

So why is there such a weak response of the acoustic rays to the tides off eastern Australia? Inspection of Figure 2, indicates that the high variability in the sound speed does not follow the spring-neap cycle or the daily cycle. So tides are causing changes, but so are eddies and currents and their effects seem to be overpowering the weak tidal effects. Alternatively, the sensitivity of the metrics could be insufficient to identify the differences. In conclusion, the weak internal wave climate off New South Wales appears insufficient to significantly impact acoustic propagation in a significant and predictable pattern like the strong internal tides of Ombai Strait in the Indonesian seas. Future work should focus on including solar radiation in the tidal simulation and improving the metrics to identify different acoustic ray behavior. After improvement of the metrics, other regions with stronger internal tides and waves should be investigated.

ACKNOWLEDGEMENTS

We would like to acknowledge the financial support from a Defence Related Research Grant from UNSW Canberra.

REFERENCES

1. Cooper, J, An investigation into the effects of internal tides on acoustic propagation in the Indonesian seas, Honours thesis, University of New South Wales Canberra, 2011.
2. Duda, TF, Identifying and meeting new challenges in shallow-water acoustics, Proceedings of Acoustics, 2013, 17-20 Nov 2013, Victor Harbour, Australia, p.1-8.
3. Dushaw, BD, Colosi, JA, Ray tracing for ocean acoustic tomography, Applied Physics Laboratory Univ. of Washington, Technical Memorandum APL-UW TM 3-98, 1998; 31 pp., staff.washington.edu/dushaw/epubs/Tech_Report_Final.pdf
4. Fofanoff, P, Millard, RC Jr, UNSEACO, Algorithms for computation of fundamental properties of seawater, UNSESCO Tech. Pap. In Marine Science No. 44, 55 pp.
5. Frosh, RA, Underwater Sound: Deep-Ocean Propagation, Science, 146, p. 889-894, 1964.
6. Hartlipp, P S, Robertson, R Internal tides off the eastern Australian coast: A comparison to observations, in preparation for Journal of Geophysical Research- Oceans, 2014.
7. Jones, AD, Zinoviev, A, Greening, MV, A study of the effects on transmission loss of water column features as modelled for an area off the east Australian coast, Proceedings of Acoustics, 2013, 17-20

Nov 2013, Victor Harbour, Australia, p.1-7.